RSC Advances

PAPER

View Article Online
View Journal | View Issue

Cite this: *RSC Adv.*, 2017, **7**, 25025

New insights on the dynamics of the γ-Fe/α-Fe phase-transition inside iron-filled carbon nanotubes†

Filippo S. Boi,*[a] Yuzhong Hu[a] and Jiqiu Wen[b]

Received 16th March 2017
Accepted 3rd May 2017

DOI: 10.1039/c7ra03144k

rsc.li/rsc-advances

One of the challenges in the field of carbon nanotubes (CNTs) is the encapsulation of a single crystalline phase of ferromagnetic α-Fe. The formation of additional γ-Fe and Fe_3C phases during CNT-growth generally limits the direct encapsulation of these crystals in the form of a single phase. A solution, the use of post-synthesis annealing, has been considered; however oxidation of the encapsulated metal-phases is commonly found due to the elevated temperatures (*T*) necessary for the phase-conversion. Here we investigate the dynamics of γ-Fe to α-Fe transition by *T*-dependent X-ray diffraction in vacuum. We show that a direct γ-Fe to α-Fe transition is present already below 200 °C and becomes significantly fast in the *T*-range of 300–399 °C. In such a *T*-range no metal oxidation is found. Rietveld refinement analyses also show that a *T*-dependent increase in the unit-cell *c*-axis value of the graphitic CNT-walls is present.

Introduction

In the last decade carbon nanotubes (CNTs) have attracted great attention in the field of nanotechnology thanks to their exceptional physical and chemical properties.[1–3] The great chemical stability makes these structures ideal to be employed as nano-sized containers for the encapsulation of specific materials of interest.[4–14] These important characteristics make CNTs ideal candidates for numerous applications in the field of nano-medicine as well as in the field of sensors and semiconductor technology.[4] One of the most interesting types of materials encapsulated inside CNTs consists of transition metals or alloys with ferromagnetic properties.[4–16] In particular Fe-based single crystals like α-Fe and Fe_3C have attracted great attention owing to the high shape and magnetocrystalline anisotropy properties that these ferromagnets exhibit in nanometer scale.[4–16] The CNTs shells can indeed chemically passivate the encapsulated nanowires and allow retaining long-term magnetic properties. Owing to the potentially exceptional saturation magnetization properties, α-Fe is generally considered one of the most valuable magnetic phases to be encapsulated inside CNTs in the form of continuous nanowires.[9,15–19] Up to now, several strategies have been attempted for the encapsulation of this phase in the form of pure single crystal. These methods are based on the evaporation and pyrolysis of a metallocene precursor (ferrocene). However, the formation of additional Fe-based phases during the CNTs growth, namely γ-Fe and Fe_3C in the form of concentrical-phases or isolated single crystals has limited the encapsulation of a single α-Fe phase.[9,15–19] In the attempt to maximize the quantity of α-Fe, a post-synthesis heating-treatment has been frequently considered[15] since bulk γ-Fe can decompose into α-Fe and Fe_3C below 727 °C in a process involving the 9% of volume expansion.[20,21] Interestingly Leonhardt *et al.* reported that a post-synthesis annealing of approximately 20 h can allow the conversion of the additional Fe-phases above into a single α-Fe phase at annealing temperatures of 645 °C in a Ar/H_2 flow.[15] However an unusual oxidation process leading to the decomposition of the CNTs and subsequent oxidation has been also reported for temperatures of approximately 675 °C and 500 °C.[15,16] In the attempt to overcome the oxidation problem mentioned above, the use of high Ar/ferrocene flow rate has been proposed.[19] However, the presence of a polycrystalline arrangement in the encapsulated crystals has limited the enhancement of the α-Fe coercive properties.[19] A recent report by Peci *et al.* has also shown that low-vapour flow rates can be beneficial for the control of the α-Fe filling rate inside CNTs-arrays,[18] however the presence of numerous oxide phases as synthesis by-products and the necessity of post-synthesis annealing treatments still limits the use of this method. In addition Fe_3C has been reported to decompose into α-Fe and graphitic carbon when in contact with the graphitic walls of the CNTs at temperatures of approximately 500–550 °C.[16,21] However the use of such temperature range for long-annealing processes is still limited by the above mentioned oxidation effect. Further understanding of the γ-Fe/α-Fe phase transition is therefore required in order to achieve

[a]College of Physical Science and Technology, Sichuan University, Chengdu, China. E-mail: f.boi@scu.edu.cn

[b]Analytical and Testing Center, Sichuan University, Chengdu, China

† Electronic supplementary information (ESI) available. See DOI: 10.1039/c7ra03144k

a complete phase-conversion without damaging the CNTs-structure. Interestingly, recent reports by Boi *et al.*[22–24] have shown that the use of a low evaporation temperature in the order of 70 °C of the chosen dichlorobenzene/ferrocene precursors, in presence of high vapour flow rates of approximately 100 ml min^{-1} can allow the synthesis of CNTs buckypaper films filled with large quantities of γ-Fe and α-Fe phases.[24]

In this work we investigate the experimental conditions necessary for the achievement of γ-Fe to α-Fe conversion without CNT damage by temperature dependent X-ray diffraction experiments in vacuum. Surprisingly we find that the conversion of the γ-Fe phase into α-Fe starts at temperatures below 200 °C and becomes significantly fast in the temperature range of 300–399 °C. We therefore demonstrate that these phase transitions can be achieved at temperatures much lower than those reported in literature. In addition, no oxidation of the annealed CNTs films is found. By using theoretical analyses through Rietveld refinements methods, we also find that a significant increase in the *c*-axis value of the graphitic CNT-walls is present at the temperature of 399 °C. Such increase implies that the distance between the graphitic lattice-planes of the CNT increases with the increase of the temperature, leading to a consequent relaxation of the high pressure γ-Fe into a α-Fe phase. These observations have a great significance since imply that the main parameter to consider for the γ-Fe to α-Fe conversion is the change of the multiwall CNT *c*-axis with the increase of the annealing-temperature.

Experimental

The synthesis of the CNTs buckypaper films used for the temperature dependent X-ray diffraction analyses was achieved by evaporation and pyrolysis of ferrocene/dichlorobenzene mixtures (1.5 g of ferrocene, 0.15 ml of dichlorobenzene) at the evaporation temperature of approximately 80–90 °C and pyrolysis temperature of 900 °C inside a quartz tube CVD reactor of length 1.5 m and inner diameter of approximately 40 mm under an Ar flow of 100 ml min^{-1}.[24] The annealing experiments were performed with a Rigaku Smartlab X-ray diffractometer (40 kV) at the temperatures of 25 °C, 100 °C, 200 °C, 300 °C, 399 °C in vacuum values below 7 Pa (for approximately 4 hours). The sample was then cooled down by fast cooling through the use of liquid nitrogen. Similar annealing conditions were used also for comparative experiments on as purchased hollow CNTs. A 200 kV American FEI Tecnai G2F20 was employed to obtain transmission electron microscopy (TEM) images. The magnetic measurements were performed at room temperature with a vibrating sample magnetometer (VSM) (Quantum Design).

Results and discussion

A typical example of a X-ray diffractogram of the as-grown buckypaper before the annealing stage is shown in Fig. 1 with red colour. The presence of multiwall CNTs was revealed by the observation of a diffraction peak in the region of 26 degrees 2θ.

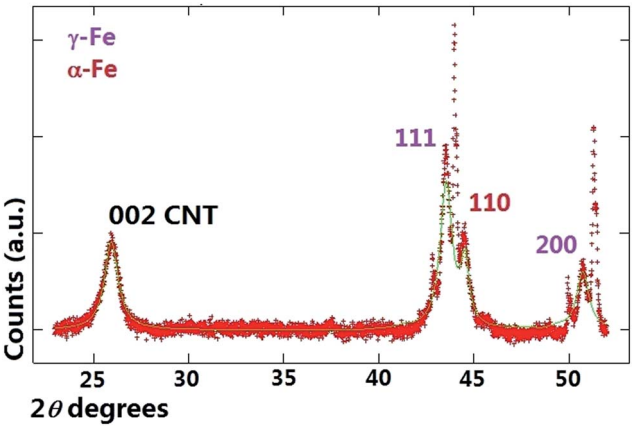

Fig. 1 X-ray diffractogram (red line) and Rietveld refinement (green line) of the as grown buckypaper before the annealing stage at 25 °C.

The presence of the γ-Fe and α-Fe phases was revealed by the observation of three diffraction peaks corresponding to the 111 and 200 reflections of γ-Fe and to the 110 reflection of α-Fe respectively (see Fig. 1). The Rietveld refinement method[25] was then used in order to estimate the unit cell parameters and relative abundance of the phases encapsulated inside the CNTs core. Note that additional unlabeled diffraction peaks are also present in Fig. 1 however those are due to the signal of the used substrate in the diffractometer. The theoretical fit of the diffractogram is represented in green colour. The unit cell parameters extracted from the Rietveld refinement were as follows; γ-Fe $a = b = c$: 0.3602 nm, α-Fe $a = b = c$: 0.2880 nm and graphitic CNT-walls $a = b$: 0.2513 nm and c: 0.6878 nm. The relative abundance of the phases comprised in the sample were: 77% graphitic carbon (comparable with that measured in ref. 24) with space group $P6_3/mmc$ (ICSD crystal database card 53781), 17% of γ-Fe (COD crystal database card 9008469) and 6% of α-Fe (COD crystal database card 1100108). Rescaling with respect to the metal phases is possible to obtain 74% of γ-Fe and 26% of α-Fe. The annealing experiment with the diffractometer mentioned above was then considered in order to investigate the minimum temperature necessary for the conversion of the γ-Fe phase into α-Fe. The attention was firstly focused on possible changes of the multiwall CNT-structure during the annealing process with the increase of the temperature.

As shown in Fig. 2A and B at first glance no significant changes in the position of the multiwall CNTs peak is observed in the interval of 25 °C to 100 °C. Instead, a small shift of the multiwall CNT-peak toward lower values of degrees 2θ is observed at the temperature of 200 °C (see Fig. 2C). The changes in the graphitic unit cell parameter were as follows; at 100 °C $a = b$: 0.2565 nm, and c: 0.6883 nm. Instead at 200 °C the measured graphitic CNT unit cell parameter were as follows; $a = b$: 0.2575 nm and c: 0.6887 nm. It is interesting to notice that a significant increase in the value of the graphitic *c*-axis is present. Further analyses were then performed on the diffraction peaks measured at the temperatures of 300 °C and 399 °C. The results of these analyses are shown in Fig. 3A and B. By using the Rietveld refinement method, in this case the following

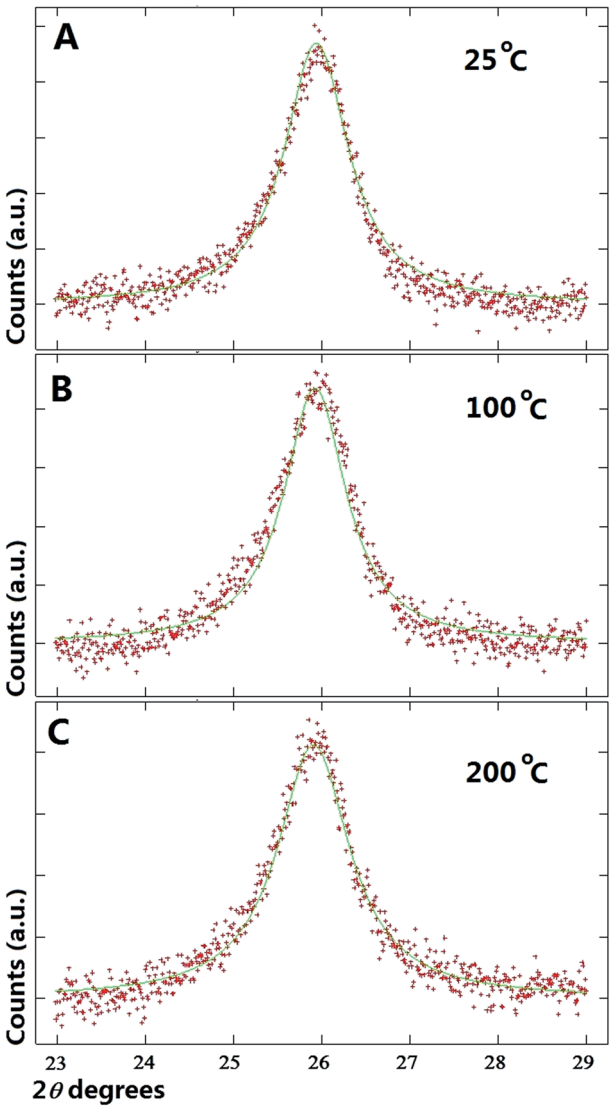

Fig. 2 (A–C), X-ray diffractograms (red line) and Rietveld refinements (green line) of the as grown buckypaper showing the graphitic CNT peak at the temperatures of 25 °C, 100 °C and 200 °C.

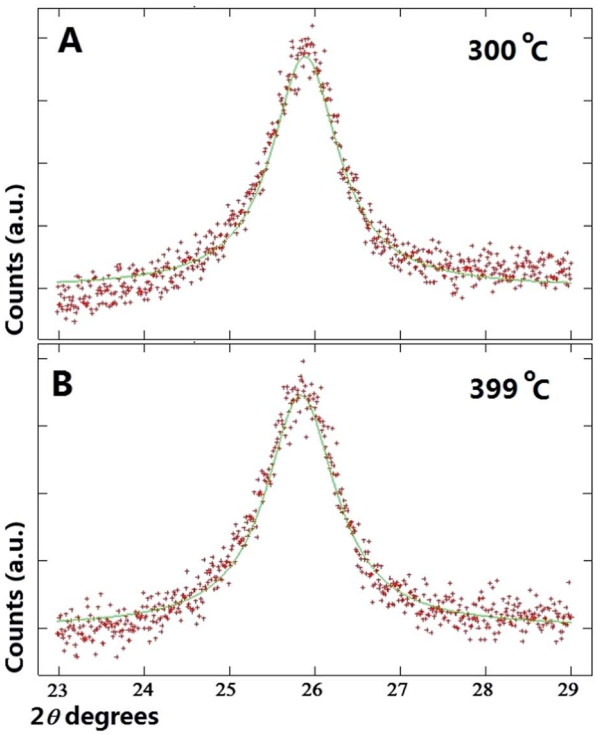

Fig. 3 (A and B), X-ray diffractograms (red line) and Rietveld refinements (green line) of the as grown buckypaper showing the graphitic CNT peak at the temperatures of 300 °C and 399 °C. See also ESI Fig. 2.†

graphitic unit-cell parameter were measured; $a = b$: 0.2577 nm and c: 0.6893 nm at 300 °C and $a = b$: 0.2579 nm and c: 0.6905 nm at 399 °C. Interestingly it is important to notice that a clear increase in the value of the c-axis is found with the increase of the temperature. Such transition can be clearly observed also in Fig. 3A and B were a shift of the CNT graphitic peak toward lower values of degrees 2θ is present. The change in the c-axis of the graphitic CNT unit-cell with temperature is shown in Fig. 4A, while the changes in the a-axis are shown in ESI.† Further investigations of the effect of annealing on the arrangement of the γ-Fe and α-Fe phases was then considered. In Fig. 4B the changes in the γ-Fe and α-Fe peaks with temperature are shown. A sudden decrease in the intensity of the 111 and 200 reflections of γ-Fe together with a peak-shift toward lower values of degrees 2θ is present in the transition from 100 °C to 200 °C. Note that with the decrease of the intensity of 111 and 200 reflections an increase in the intensity of the α-Fe 110 reflection is found. This variation in the reflection-intensities becomes clearer in the transition from 200 °C to 399 °C where a dramatic decrease in the intensity of the 111 and 200 reflections of γ-Fe is found. The quantification of the relative abundance of γ-Fe converted into α-Fe in the temperature interval of 200–399 °C was then considered by using the Rietveld refinement method. The Rietveld refinement of the diffractograms measured at 200 °C, 300 °C and 399 °C is shown in Fig. 5A–C. The following changes in the unit-cell parameters were found for γ-Fe, $a = b = c$: 0.3605 at 200 °C, $a = b = c$: 0.3615 at 300 °C and $a = b = c$: 0.3617 at 399 °C. Instead the following changes in the unit-cell parameters were found for α-Fe, $a = b = c$: 0.2880 nm at 200 °C, $a = b = c$: 0.2885 nm at 300 °C and $a = b = c$: 0.2887 nm at 399 °C. Thus, evaluating the changes in relative abundance of the encapsulated phases, a decrease in the relative abundance of γ-Fe from 68% (200 °C) to 46% (399 °C) is found. As consequence an increase in the relative abundance of α-Fe from 32% (200 °C) to 54% (399 °C) is found. An unusual decrease in the 002 carbon reflection intensity is also found despite the used vacuum conditions below 7 Pa. Such decrease could be therefore associated to the possible transformation of a small quantity of graphitic carbon into an amorphous carbon phase. Note that no oxide phases were observed in the sample. In addition it is very important to notice that no formation of additional Fe_3C crystals is found as a result of γ-Fe decomposition. The γ-Fe to α-Fe transition is therefore found to be a direct transition possibly induced by the change in the c-axis value of the graphitic-CNT

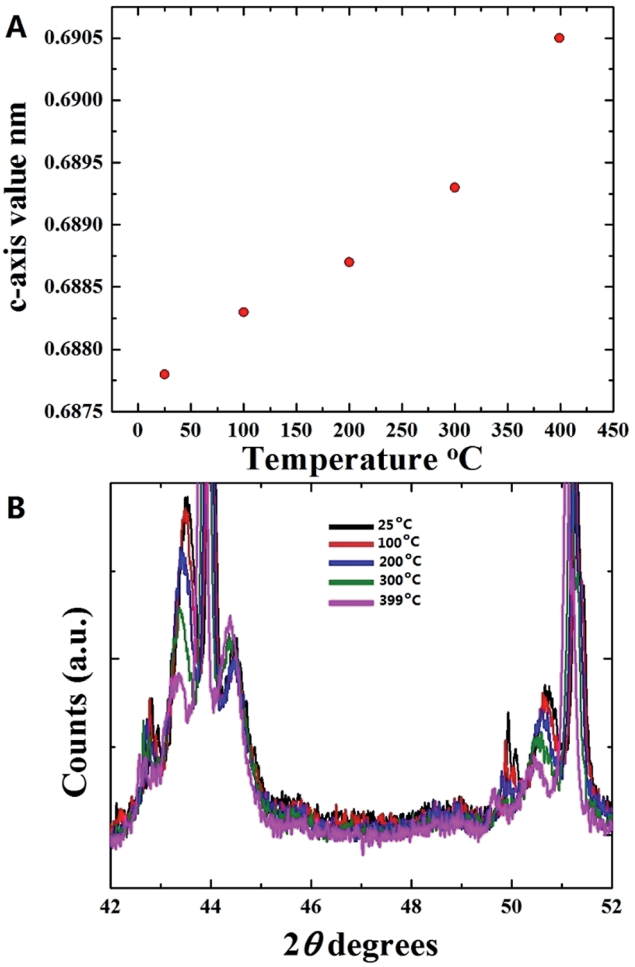

Fig. 4 In (A) the variation of the *c*-axis of the graphitic CNT unit-cell with temperature is shown. In (B) the variation of the diffraction-peaks position for the γ-Fe and α-Fe phases with temperature is shown. See ESI Fig. 3† for the final XRD pattern obtained after cooling with liquid nitrogen.

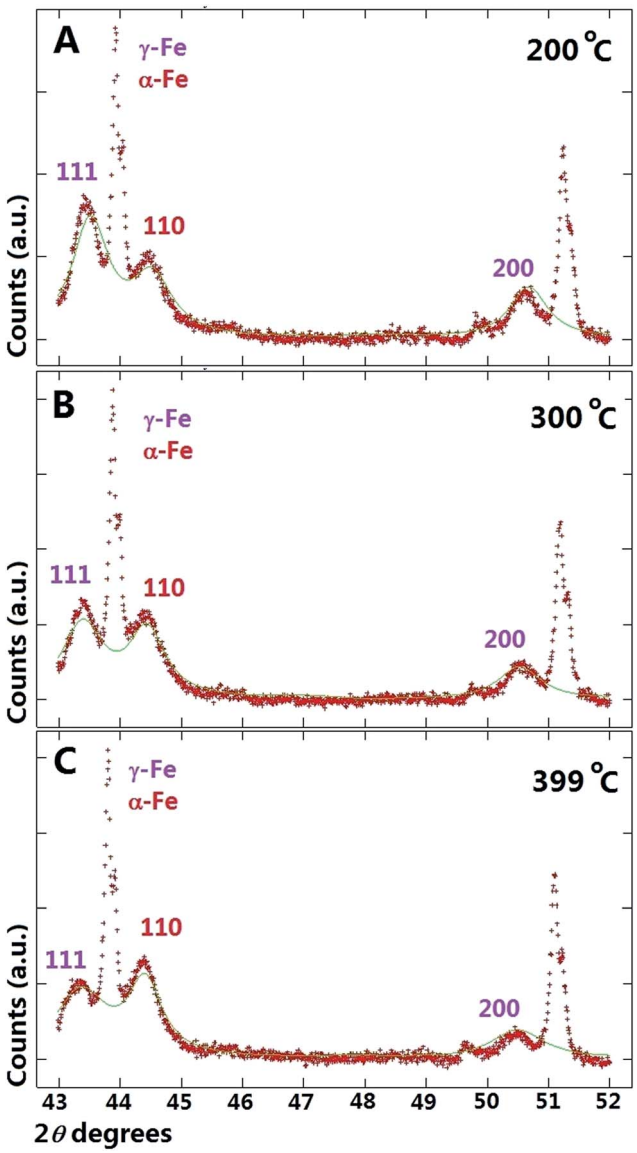

Fig. 5 (A–C), X-ray diffractograms (red line) and Rietveld refinements (green line) of the as grown buckypaper showing the variation of the diffraction-peaks position for the γ-Fe and α-Fe phases with temperature at the temperatures of 200 °C, 300 °C and 399 °C.

with temperature and therefore from a possible decrease in the pressure applied by the CNTs walls into the encapsulated crystals.

Our observations exclude the presence of a decomposition process which would then yield α-Fe and Fe_3C. These findings have a great significance in the field of Fe-filled CNTs since can allow the manipulation of CNTs-filling material without oxidation problems at much lower temperatures than those used in previous reports. In order to further verify these observations, additional temperature dependent XRD measurements were then performed in hollow CNTs samples (see Fig. 9 ESI† for TEM micrograph). Typical XRD analyses performed in these hollow CNTs samples (in similar vacuum conditions) at the temperatures of 25 °C, 200 °C and 400 °C are shown in Fig. 6–8 ESI.† In order to compare the obtained results with those shown above for the Fe-filled CNTs sample, the use of Rietveld refinement was considered also in this case. The plots showing the variation of the *c*-axis and *a*-axis of the CNTs graphitic unit-cell with temperature are shown in Fig. 4 and 5 ESI.† Curiously we find that also in this case an increase in the *c*-axis is found with the temperature. However this change in graphitic CNT unit cell appears to be different with respect to that observed in the case of the Fe-filled CNTs sample. In particular a major difference is observed in the case of the *a*-axis, as shown in Fig. 5 ESI.† The graphitic CNT unit cell values extracted with the Rietveld refinement were as follow: for the measurements performed at 25 °C $a = b$: 0.2485 nm and c: 0.6890 nm. For the measurements performed at 200 °C $a = b$: 0.2486 nm and c: 0.6893 nm. Instead for the measurements performed at 400 °C, $a = b$: 0.2494 nm and c: 0.6910 nm.

In order to further verify the encapsulation of the Fe-based crystals within the CNT-capillary, further cross-sectional investigations were performed with transmission electron microscopy (TEM). The presence of Fe-crystals within the CNT-core was confirmed by TEM micrographs in Fig. 6A and B. These analyses

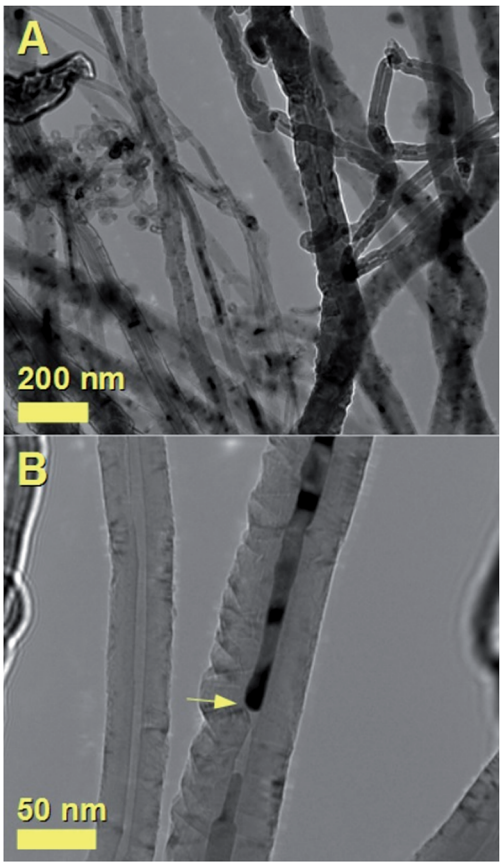

Fig. 6 TEM micrographs showing in (A and B) the morphology of the as grown CNTs filled with large quantities of γ-Fe/α-Fe crystals. In (B) the yellow arrow indicates a cross-sectional region of the CNT where a high stress seems to be present. The black region within the CNT-core represents the encapsulated Fe-crystal.

revealed also possible presence of stress within the CNTs-structure. In addition, in order to verify the possible changes in the magnetization between the un-annealed and annealed samples, VSM measurements were performed at 300 K. As shown in Fig. 7, these measurements confirmed the presence of an increase in the magnetization, from the value of approximately 29 emu g^{-1} (before annealing), to the value of approximately 37 emu g^{-1} (after annealing). Instead no changes in the coercivity were found (coercivity of approximately 293 Oe).

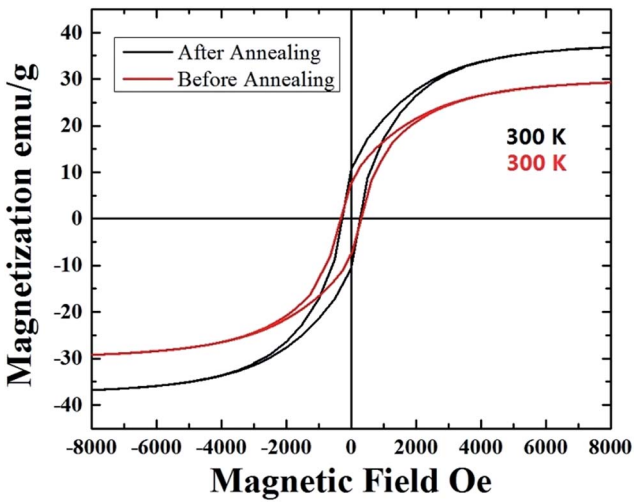

Fig. 7 Room temperature hysteresis loops of the as grown (red hysteresis) and vacuum-annealed (black hysteresis) samples.

Conclusion

In conclusion we have investigated the dynamics of γ-Fe to α-Fe conversion by temperature dependent X-ray diffraction experiments in vacuum. Our results show that the conversion of the γ-Fe phase into α-Fe starts at temperatures below 200 °C and becomes significantly fast in the temperature range of 300–399 °C. These results are much different with respect to those reported in literature where the use of much higher annealing temperatures has been reported to induce the oxidation of the filled CNTs structures. Note that in our experiment, no oxidation process of the annealed CNTs films is found. By using theoretical analyses through Rietveld refinements methods we find that a significant increase in the *c*-axis value of the graphitic CNT-walls is present with the increase of the temperature from the value of 0.6878 nm at 25 °C up to the value of 0.6905 nm at the temperature of 399 °C. Such increase implies that the distance between the graphitic lattice-planes of the CNT can possibly increase with the increase of the temperature, leading to a consequent direct relaxation of the high pressure γ-Fe phase into a α-Fe phase at much lower temperatures than those previously reported in literature. These structural changes were compared also with those of hollow CNTs. The observed phase transitions in the encapsulated Fe phases were also confirmed by additional magnetization analyses.

Acknowledgements

We acknowledge Prof. Gong Min for his continuous support and the National Natural Science Foundation of China Grant No. 11404227.

Notes and references

1 S. Iijima and T. Ichihashi, *Nature*, 1993, **363**, 603.
2 S. Iijima, *Nature*, 1991, **354**, 56.
3 M. S. Dresselhaus, *Nat. Mater.*, 2004, **3**, 665.
4 U. Weissker, S. Hampel, A. Leonhardt and B. Buchner, *Materials*, 2010, **3**, 4387.
5 A. Leonhardt, S. Hampel, C. Muller, I. Monch, R. Koseva, M. Ritschel, D. Elefant, K. Biedermann and B. Buchner, *Chem. Vap. Deposition*, 2006, **12**, 380.
6 A. Leonhardt, M. Ritschel, R. Kozhuharova, A. Graffa, T. Muhl, R. Huhle, I. Monch, D. Elefant and C. M. Schneider, *Diamond Relat. Mater.*, 2003, **12**, 790.
7 U. Weissker, M. Loffler, F. Wolny, M. U. Lutz, N. Scheerbaum, R. Klingeler, T. Gemming, T. Muhl, A. Leonhardt and B. Buchner, *J. Appl. Phys.*, 2009, **106**, 054909.

8 H. Terrones, F. Lopez-Urias, E. Munoz-Sandoval, J. A. Rodriguez-Manzo, A. Zamudio, A. L. Elias and M. Terrones, *Solid State Sci.*, 2006, **8**, 303.
9 S. Hampel, A. Leonhardt, D. Selbmann, K. Biedermann, D. Elefant, C. Muller, T. Gemming and B. Buchner, *Carbon*, 2006, **44**, 2316.
10 A. Morelos-Gomez, F. Lopez-Urias, E. Munoz-Sandoval, C. L. Dennis, R. D. Shull, H. Terrones and M. Terrones, *J. Mater. Chem.*, 2010, **20**, 5906.
11 C. Prados, P. Crespo, J. M. Gonzalez, A. Hernando, J. F. Marco, R. Gancedo, N. Grobert, M. Terrones, R. M. Walton and H. W. Kroto, *Phys. Rev. B: Condens. Matter Mater. Phys.*, 2002, **65**, 113405.
12 S. Karmakar, S. M. Sharma, M. D. Mukadam, S. M. Yusuf and A. K. Sood, *J. Appl. Phys.*, 2005, **97**, 054306.
13 C. Muller, D. Golberg, A. Leonhardt, S. Hampel and B. Buchner, *Phys. Status Solidi A*, 2006, **203**(6), 1064.
14 C. Muller, A. Leonhardt, S. Hampel and B. Buchner, *Phys. Status Solidi B*, 2006, **243**, 3091.
15 A. Leonhardt, M. Ritschel, M. Elefant, D. N. Mattern, K. Biedermann, S. Hampel, C. Muller, T. Gemming and B. Buchner, *J. Appl. Phys.*, 2005, **98**, 074315.
16 F. S. Boi, G. Mountjoy, R. M. Wilson, Z. Luklinska, L. J. Sawiak and M. Baxendale, *Carbon*, 2013, **64**, 351.
17 X. Gui, J. Wei, K. Wang, W. Wang, R. Lv, J. Chang, F. Kang, J. Gu and D. Wu, *Mater. Res. Bull.*, 2008, **43**, 3441.
18 T. Peci and M. Baxendale, *Carbon*, 2015, **98**, 519.
19 F. S. Boi, S. Maugeri, J. Guo, M. Lan, S. Wang, J. Wen, *et al.*, *Appl. Phys. Lett.*, 2014, **105**, 243108.
20 W. D. Callister, *Fundamentals of Materials Science and Engineering*, John Wiley and Sons, 2007.
21 A. Schneider, *Corros. Sci.*, 2002, **44**, 2353.
22 J. Guo, Y. He, S. Wang and F. S. Boi, *Carbon*, 2016, **102**, 372.
23 F. S. Boi, J. Guo, S. Wang, Y. He, G. Xiang, X. Zhang, *et al.*, *Chem. Commun.*, 2016, **52**, 4195.
24 F. S. Boi, Y. Hu, S. Wang and Y. He, *RSC Adv.*, 2016, **6**, 69226.
25 A. L. Larson and R. Von Dreele, *GSAS, General Structure Analysis System Report LAUR 86-748*, Los Alamos National Laboratory, Los Alamos USA, 1986.